VoxelMap++ Supplementary Material

Yuan You and Yifei Yuan

October 16, 2023

1 Detailed Deviation about 3DOF Plane Estimation

Assuming a group of coplanar LiDAR points ${}^W\mathbf{p}_i, (i = 1, \cdots, N)$ with covariance $\Sigma_{{}^W\mathbf{p}_i}$. Plane can be extracted from this point cloud parameterized as (1) by normalizing along the z-component (main-axis).

$$ax + by + z + d = 0 \tag{1}$$

Since all ${}^W\mathbf{p}_i$ are co-planar satisfied (1). Then, stack all constrains about the plane, the least squares optimization function can be constructed as (2).

$$\begin{bmatrix} x_1 & y_1 & 1 \\ x_2 & y_2 & 1 \\ \vdots & \vdots & \vdots \\ x_n & y_n & 1 \end{bmatrix} \mathbf{n} = \begin{bmatrix} -z_1 \\ -z_2 \\ \vdots \\ -z_n \end{bmatrix} \tag{2}$$

After a series of identical deformations shown in (3)(4).

$$\begin{bmatrix} x_1 & x_2 & \cdots & 1 \\ y_1 & y_2 & \cdots & 1 \\ 1 & 1 & \cdots & 1 \end{bmatrix} \begin{bmatrix} x_1 & y_1 & 1 \\ x_2 & y_2 & 1 \\ \vdots & \vdots & \vdots \\ x_n & y_n & 1 \end{bmatrix} \mathbf{n} = \begin{bmatrix} x_1 & x_2 & \cdots & 1 \\ y_1 & y_2 & \cdots & 1 \\ 1 & 1 & \cdots & 1 \end{bmatrix} \begin{bmatrix} -z_1 \\ -z_2 \\ \vdots \\ -z_n \end{bmatrix} \tag{3}$$

$$\begin{bmatrix} \sum x_i x_i & \sum x_i y_i & \sum x_i \\ \sum x_i y_i & \sum y_i y_i & \sum y_i \\ \sum x_i & \sum y_i & N \end{bmatrix} \mathbf{n} = - \begin{bmatrix} \sum x_i z_i \\ \sum y_i z_i \\ \sum z_i \end{bmatrix} \tag{4}$$

A closed-form solution of $\mathbf{n}$ can be obtained (5). $\mathbf{A}^*$ is the adjugate matrix of $\mathbf{A}$, $A_{ij} = (-1)^{i+j} M_{ij}$ is the algebraic cofactor of $\mathbf{A}$, the expression of $\mathbf{A}$ and $\mathbf{e}$ is shown as (6)(7).

$$\mathbf{n} = \frac{\mathbf{A}^*}{|\mathbf{A}|}\mathbf{e} \tag{5}$$

$$\mathbf{A} = \begin{bmatrix} \sum x_i x_i & \sum x_i y_i & \sum x_i \\ \sum x_i y_i & \sum y_i y_i & \sum y_i \\ \sum x_i & \sum y_i & N \end{bmatrix}, \mathbf{A}^* = \begin{bmatrix} A_{11} & A_{12} & A_{13} \\ A_{21} & A_{22} & A_{23} \\ A_{31} & A_{32} & A_{33} \end{bmatrix} \tag{6}$$

$$\mathbf{e} = \begin{bmatrix} -\sum x_i z_i & -\sum y_i z_i & -\sum z_i \end{bmatrix}^T \tag{7}$$

Based on the closed-form solution of $\mathbf{n}$, the uncertainty of the plane is hence

$$\mathbf{\Sigma_n} = \sum_i^N \frac{\partial \mathbf{n}}{\partial {}^W\mathbf{p}_i} \mathbf{\Sigma}_{{}^W\mathbf{p}_i} \frac{\partial \mathbf{n}}{\partial {}^W\mathbf{p}_i}^T \tag{8}$$

Where the covariance matrix $\mathbf{\Sigma_n}$ is the uncertainty of plane 3DOF representation, which is calculated from the covariance matrix of the points on the plane $\mathbf{\Sigma}_{{}^W\mathbf{p}_i}$. The detailed deviation about $\frac{\partial \mathbf{n}}{\partial {}^W\mathbf{p}_i}$ is a little bit complicated related to $\frac{\partial \mathbf{A}^*\mathbf{e}}{\partial {}^W\mathbf{p}_i}$ and $\frac{\partial |\mathbf{A}|}{\partial {}^W\mathbf{p}_i}$ shown as (9)(10)(11).

$$\frac{\partial \mathbf{n}}{\partial^W \mathbf{p}_i} = \frac{1}{|\mathbf{A}|^2}\left(\frac{\partial \mathbf{A}^*\mathbf{e}}{\partial^W \mathbf{p}_i}|\mathbf{A}| - \frac{\mathbf{A}^*\mathbf{e}\partial|\mathbf{A}|}{\partial^W \mathbf{p}_i}\right) \tag{9}$$

$$\mathbf{A}^*\mathbf{e} = -\begin{bmatrix} A_{11}\sum x_i z_i + A_{12}\sum y_i z_i + A_{13}\sum z_i \\ A_{21}\sum x_i z_i + A_{22}\sum y_i z_i + A_{23}\sum z_i \\ A_{31}\sum x_i z_i + A_{32}\sum y_i z_i + A_{33}\sum z_i \end{bmatrix} = \begin{bmatrix}\lambda_1 \\ \lambda_2 \\ \lambda_3\end{bmatrix} \tag{10}$$

$$|\mathbf{A}| = N\sum x_i^2 \sum y_i^2 + 2\sum x_i y_i \sum x_i \sum y_i - N(\sum x_i y_i)^2 - (\sum x_i)^2 \sum y_i^2 - (\sum y_i)^2 \sum x_i^2 \tag{11}$$

In (10)(11), each term is related to ${}^W\mathbf{p}_i$, the expressions of $\frac{\partial \mathbf{A}^*\mathbf{e}}{\partial^W \mathbf{p}_i}$ and $\frac{\partial|\mathbf{A}|}{\partial^W \mathbf{p}_i}$ can be determined as (12)(13)(14) following the chain derivation rule.

$$\frac{\partial \mathbf{A}^*\mathbf{e}}{\partial^W \mathbf{p}_i} = \begin{bmatrix} \frac{\partial \lambda_1}{\partial^W \mathbf{p}_i} & \frac{\partial \lambda_1}{\partial^W \mathbf{p}_i} & \frac{\partial \lambda_1}{\partial^W \mathbf{p}_i} \end{bmatrix} \tag{12}$$

$$\frac{\partial \lambda_j}{\partial^W \mathbf{p}_i} = \begin{bmatrix} \frac{\partial A_{j1}}{\partial x_i}\sum x_i z_i + \frac{\partial A_{j2}}{\partial x_i}\sum y_i z_i + \frac{\partial A_{j3}}{\partial x_i}\sum z_i + A_{j1} z_i \\ \frac{\partial A_{j1}}{\partial y_i}\sum x_i z_i + \frac{\partial A_{j2}}{\partial y_i}\sum y_i z_i + \frac{\partial A_{j3}}{\partial y_i}\sum z_i + A_{j2} y_i \\ \frac{\partial A_{j1}}{\partial z_i}\sum x_i z_i + \frac{\partial A_{j2}}{\partial z_i}\sum y_i z_i + \frac{\partial A_{j3}}{\partial z_i}\sum z_i + A_{j1} x_i + A_{j2} y_i + A_{j3} \end{bmatrix}^T \tag{13}$$

$$\frac{\partial|\mathbf{A}|}{\partial^W \mathbf{p}_i} = 2\begin{bmatrix} N x_i \sum y_i^2 + \sum y_i(\sum x_i y_i + y_i \sum x_i) - N\sum x_i y_i - \sum x_i \sum y_i^2 - x_i \sum y_i^2 \\ N y_i \sum x_i^2 + \sum x_i(\sum x_i y_i + x_i \sum y_i) - N\sum x_i y_i - \sum y_i \sum x_i^2 - y_i \sum x_i^2 \\ 0 \end{bmatrix}^T \tag{14}$$

Because $\mathbf{A}$ is unrelated to z_i in ${}^W\mathbf{p}_i$, $\frac{\partial \lambda_j}{\partial^W \mathbf{p}_i}$ can be simplified as (15). $\frac{\partial A_{ij}}{\partial^W \mathbf{p}_i}$ is the jacobian of algebraic cofactor of $\mathbf{A}$ to $\partial^W \mathbf{p}_i$ shown as below. Because $\mathbf{A}$ and $\mathbf{A}^*$ is the symmetric matrix, which means $A_{ij} = A_{ji}$ and $\frac{\partial A_{ij}}{\partial^W \mathbf{p}_i} = \frac{\partial A_{ji}}{\partial^W \mathbf{p}_i}$.

$$\frac{\partial \lambda_j}{\partial^W \mathbf{p}_i} = \begin{bmatrix} \frac{\partial A_{j1}}{\partial x_i}\sum x_i z_i + \frac{\partial A_{j2}}{\partial x_i}\sum y_i z_i + \frac{\partial A_{j3}}{\partial x_i}\sum z_i + A_{j1} z_i \\ \frac{\partial A_{j1}}{\partial y_i}\sum x_i z_i + \frac{\partial A_{j2}}{\partial y_i}\sum y_i z_i + \frac{\partial A_{j3}}{\partial y_i}\sum z_i + A_{j2} y_i \\ A_{j1} x_i + A_{j2} y_i + A_{j3} \end{bmatrix}^T \tag{15}$$

$$\begin{aligned}
\frac{\partial A_{11}}{\partial^W \mathbf{p}_i} &= 2\begin{bmatrix} 0 & N y_i - \sum y_i & 0 \end{bmatrix} \\
\frac{\partial A_{12}}{\partial^W \mathbf{p}_i} &= \begin{bmatrix} -N y_i + \sum y_i & -N x_i + \sum x_i & 0 \end{bmatrix} \\
\frac{\partial A_{13}}{\partial^W \mathbf{p}_i} &= \begin{bmatrix} y_i \sum y_i - \sum y_i^2 & x_i \sum y_i + \sum x_i y_i - 2 y_i \sum x_i & 0 \end{bmatrix} \\
\frac{\partial A_{22}}{\partial^W \mathbf{p}_i} &= 2\begin{bmatrix} N x_i - \sum x_i & 0 & 0 \end{bmatrix} \\
\frac{\partial A_{23}}{\partial^W \mathbf{p}_i} &= \begin{bmatrix} -2 x_i \sum y_i + y_i \sum x_i + \sum x_i y_i & -\sum x_i^2 + x_i \sum x_i & 0 \end{bmatrix} \\
\frac{\partial A_{33}}{\partial^W \mathbf{p}_i} &= 2\begin{bmatrix} x_i \sum y_i - y_i \sum x_i y_i & y_i \sum x_i - x_i \sum x_i y_i & 0 \end{bmatrix}
\end{aligned} \tag{16}$$

By substituting (15)(16) into (12)(14), $\frac{\partial \mathbf{n}}{\partial^W \mathbf{p}_i}$ in (9) can be obtained. Finally, by summing all covariance related to ${}^W\mathbf{p}_i$, the 3DOF covariance expression of the plane in (8) can be obtained.

2 Experiment in Dynamic Crowded Intersection

In order to demonstrate the robustness of VoxelMap++ in typical dynamic scenarios, we conducted supplementary experiments on dynamic scenarios in this section. The experiment scene is the entrance of Liren Building in UESTC, which is a crowded intersection show in Fig.1. Due to the lack of hardware for GNSS-IMU systems with real-time kinematic signals or other ground truth. We use end- to-end errors, which are defined as the difference between the start point and terminal point, to compare the accuracy of different algorithms.

(a) Dynamic experiment environment

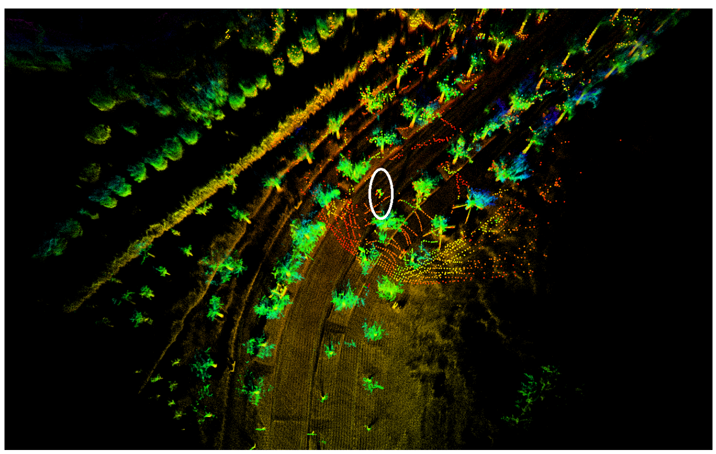

(b) When building the map, the objects inside the white circle are moving

Figure 1: Experiments on crowded intersection

As shown in Table.1, our proposed VoxelMap++, like other algorithms, has robustness in dynamic scenarios and will not diverge easily.

Table 1: end-to-end error(meters) on dynamic crowded intersection

Sequence	loop1	loop2
LIO-Livox	3.8780	1.1116
FAST-LIO2	3.2883	**0.0331**
Faster-LIO	0.0994	0.1423
VoxelMap	0.4940	0.0572
VoxelMap++	**0.0721**	0.0648
Route Length(m)	217.4	173.9

3 Visualization results about Plane Merging

3.1 Indoor Corridor

In VoxelMap++, due to the advantage of plane merging, the entire floor and ceiling will be merged into two large planes, thus constraining the drift on the pitch and avoiding linear cumulative errors which are shown in Fig. 8. This phenomenon is similar to the ground segmentation in LeGO-LOAM, but it is further extended to all coplanar planes. In the direction of degeneracy occurred, VoxelMap++ can merge the coplanar walls at the end of the corridor, thereby enhancing their constraints to alleviate degradation by reducing the covariance about these planes.

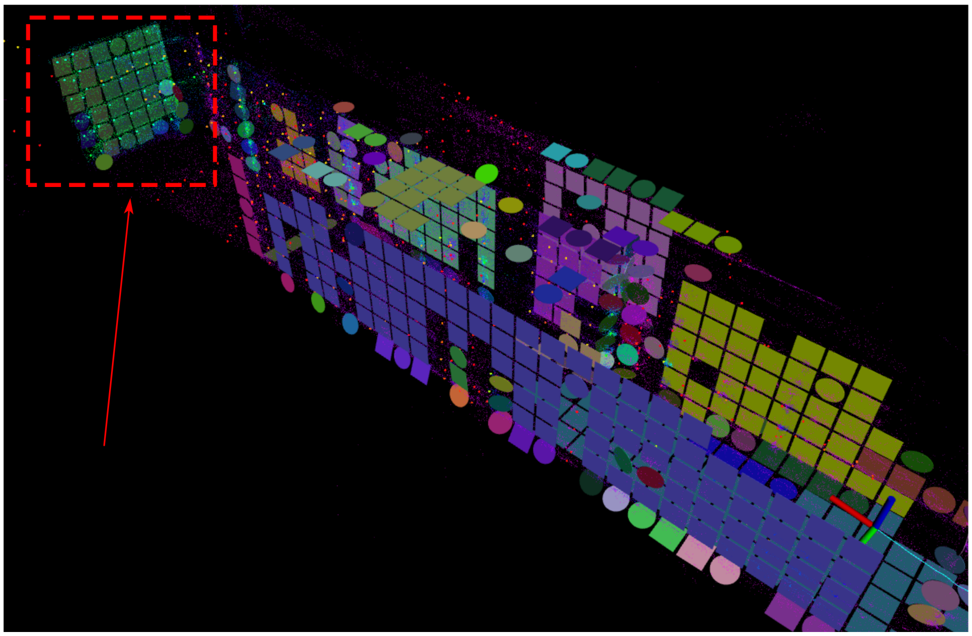

(a) Plane construction of the entire corridor

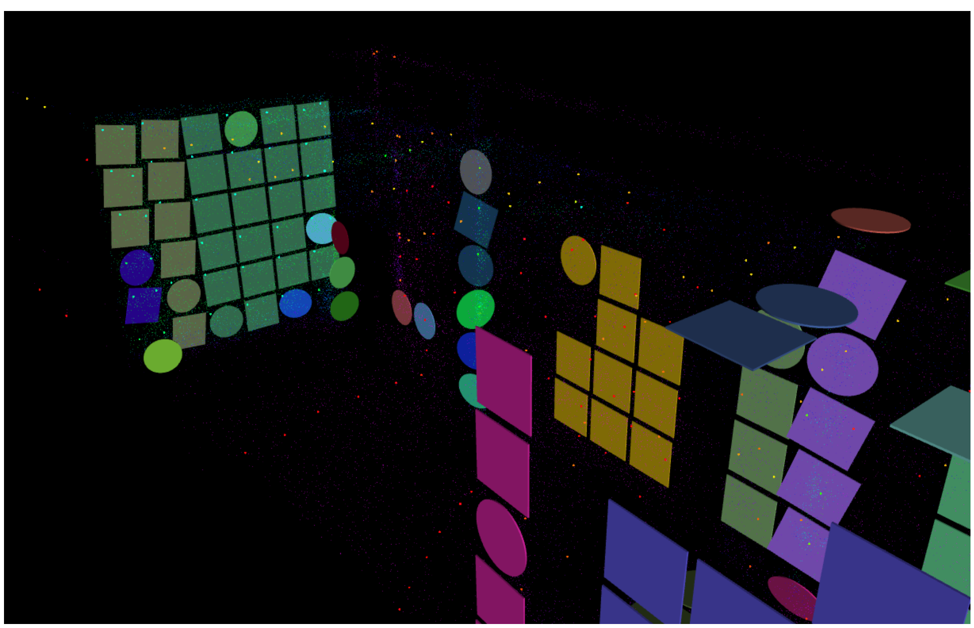

(b) Plane construction in the end of the corridor

Figure 2: Plane merging effort in the indoor degenerated corridor.

3.2 Unstructured Scene

The error detection of coplanar recognition based on the chi-square test in plane merging is relatively low, therefore it also has robustness in unstructured scenarios like VoxelMap. As shown in Fig.3, the planes on the tree are not merged incorrectly. So VoxelMap++, like VoxelMap, has robustness in unstructured scenarios.

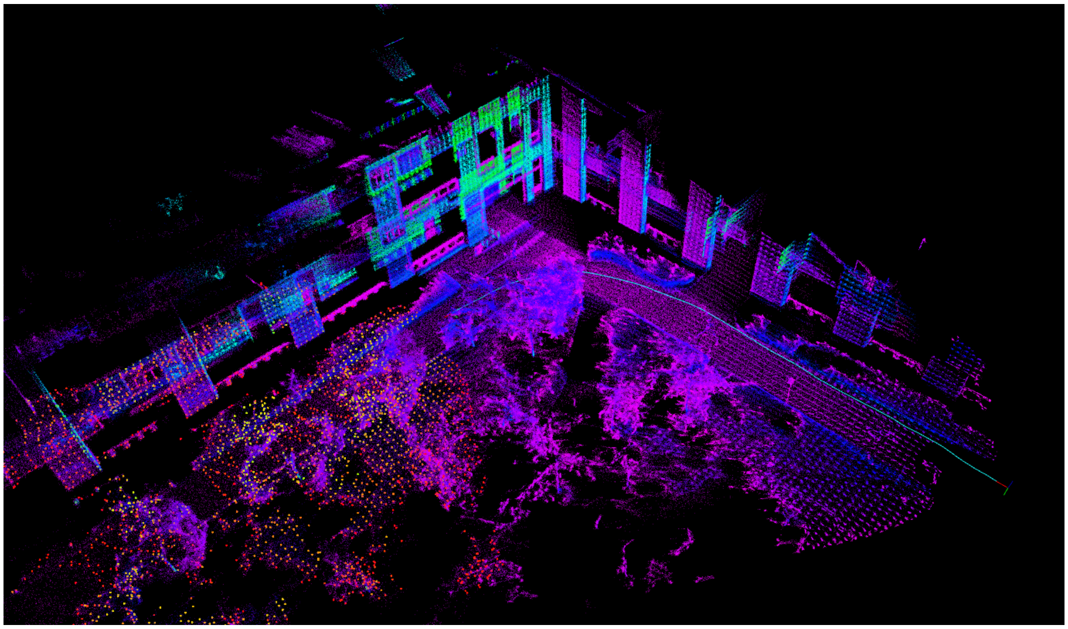

(a) PointCloud map of unstructured environment

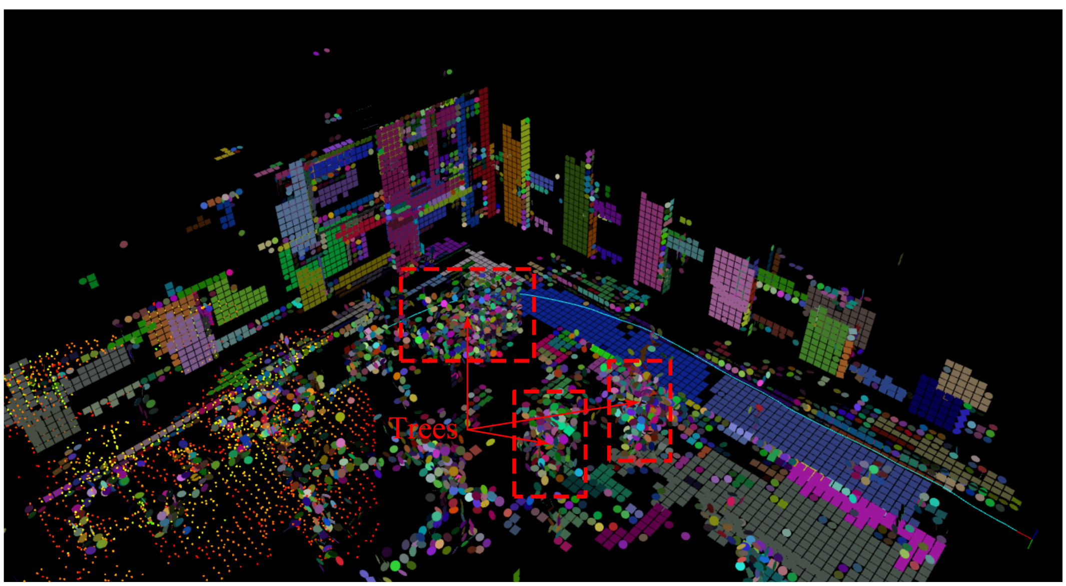

(b) Plane construction of unstructured environment

Figure 3: Plane merging effort in the unstructured scene